

# *In Silico* Interactions of Some of the Triazole Derivatives with the Main Protease of Coronavirus

Elham Salarrezaei <sup>1,\*</sup>, Kun Harismah <sup>2,\*</sup>, Mahmoud Mirzaei <sup>3,\*</sup>

<sup>1</sup> Student Research Committee, School of Advanced Technologies in Medicine, Isfahan University of Medical Sciences, Isfahan, Iran; e.salarrezaei@gmail.com (E.S.);

<sup>2</sup> Department of Chemical Engineering, Faculty of Engineering, Universitas Muhammadiyah Surakarta, Surakarta, Indonesia; kun.harismah@ums.ac.id (K.H.);

<sup>3</sup> Child Growth and Development Research Center, Research Institute for Primordial Prevention of Non-Communicable Disease, Isfahan University of Medical Sciences, Isfahan, Iran; mirzaei.res@gmail.com (M.M.);

\* Correspondence: e.salarrezaei@gmail.com (E.S.); kun.harismah@ums.ac.id (K.H.); mirzaei.res@gmail.com (M.M.);

Scopus Author ID 57216370465 (E.S.);

56982926300 (K.H.);

13204227300 (M.M.);

**Received: 6.08.2022; Accepted: 20.09.2022; Published: 31.10.2022**

**Abstract:** This work was done to assess *in silico* interactions of some of the 1,2,4-triazole derivatives with the main protease (MPro) of coronavirus to approach insights into enzymatic activity inhibition. Fifteen models of triazole derivatives (T2-T16) were investigated in this work to examine such benefits of structural modifications of T1 for approaching better ligand structures. The density functional theory (DFT) calculations indicated that the derivative ligand models were in their new characteristic specifications compared with the original T1 ligand and other T ligands. One important point was that the derivatives ligands were in higher levels of activity in comparison with the original T1 affirming the benefits of employing such structural modifications. Next, the results of molecular docking simulations indicated the potential of derivative ligands for participating in efficient interactions with the MPro target of coronavirus. As a result, the ligand models were stabilized. Their interactions with the MPro of coronavirus revealed that the investigated triazole derivatives could be considered possible inhibitors of MPro of coronavirus.

**Keywords:** triazole; coronavirus; docking; inhibition; main protease.

© 2022 by the authors. This article is an open-access article distributed under the terms and conditions of the Creative Commons Attribution (CC BY) license (<https://creativecommons.org/licenses/by/4.0/>).

## 1. Introduction

Of the occurrence of a novel coronavirus disease pandemic in late 2019 (COVID-19), almost all researchers focused on the development of a new protocol of treatment for this unknown disease [1-3]. Soon after the appearance of such a pandemic, serious negative impacts have been seen on all sides of the human life system all around the world [4-6]. Because of such a complicated issue, it has been the first research topic to provide more insights into this disease [7-9]. In this regard, developing protocols for both the prevention and medication sides of COVID-19 have been investigated by researchers, but a certain success has not yet been achieved [10-12]. To this aim, several works have been investigated to know possible treatments for COVID-19 patients; one of them has been the innovation of novel inhibitors for the main protease (MPro) of coronavirus [13-15]. Although the earlier efforts revealed some possible inhibitors for MPro, further investigations are still required to approach more insights into inhibiting the activity of this enzyme [16-18]. Accordingly, this work was performed to

recognize the possibility of inhibition of MPro by triazole derivatives. The issue of drug design, discovery, and development has been a non-stop process from the ancient era up to this time [19-21]. Accordingly, several methodologies have been employed to recognize the features of both chemical and biochemical systems to learn the benefits of investigating such systems for approaching pharmaceutical applications [22-24]. In the case of COVID-19, several efforts have been made to learn how to deal with this disease [25-27].

Triazole (Figure 1) is a starting organic material for synthesizing other organic and bioorganic compounds [28, 29]. Several organic compounds with pharmaceutical potentials have been introduced at this time [30, 31]. A series of synthesized triazole compounds (Figure 2) by an earlier work was investigated against the inhibition of MPro of coronavirus through computational methods [32, 33]. First, quantum chemical calculations and molecular docking simulations were performed to investigate features of triazole ligand molecules and their interactions with the MPro target; the results were summarized in Table 1 and Figures 2 and 3. Next, the obtained results were discussed to approach a point of assessing triazole derivatives for interacting with the MPro of coronavirus to show potentials of activity inhibitions.

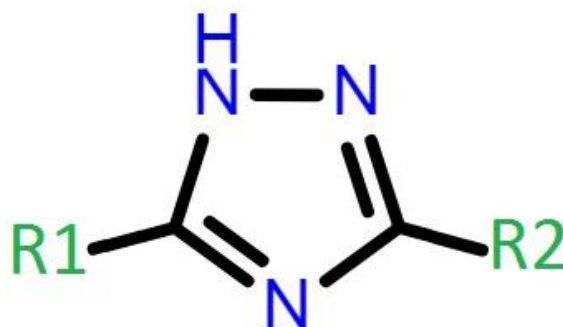


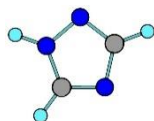
**Figure 1.** Representation of 1,2,4-triazole; R1 and R2 are the sites of derivatization.

## 2. Materials and Methods

In this work, the 3D molecular models and the computational tools and concepts were employed to perform an *in silico* investigation of some triazole derivatives' interactions with the coronavirus MPro. To this aim, fifteen derivatives of 1,2,4-triazole were extracted from earlier work [32] to be investigated as possible inhibitor ligands for the MPro target of coronavirus. As shown in Figure 1, R1 and R2 sites of triazole were substituted by other molecular groups to yield T2-T16 derivatives, which the models described in Figure 2. In the original triazole model, the hydrogen atoms substituted T1, R1, and R2. Geometries of 3D structures of ligand models were optimized, and their stabilized representations and frontier molecular orbitals patterns were shown in Figure 2, including the energetic descriptors in Table 1. The dominant frontier levels of molecular orbitals were assigned by the highest occupied and the lowest unoccupied molecular orbitals (HOMO and LUMO). The B3LYP/6-31G\* computational level of density functional theory (DFT) was used in this work as implemented in the Gaussian program [34]. Next, the 3D structure of MPro was extracted from the Protein Data Bank (6LU7) [35], and it was prepared for involvement as the target of molecular docking simulations. Afterward, molecular docking simulations of the models of ligands and targets were performed using the HDOCK web server [36]. As a consequence, the interacting bimolecular ligand-target models were found, and they were shown in Figure 3, besides including their scores in Table 1. To this point, the investigated models and their features were

recognized for further discussing the major problem of this work to learn the potentials of triazole derivatives for inhibiting the MPro of coronavirus.

T1: R1=H, R2=H



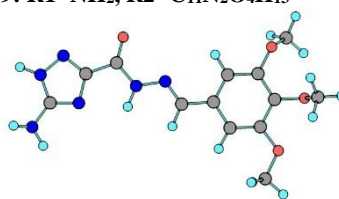
L



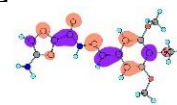
H



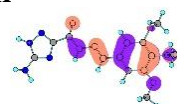
T9: R1=NH<sub>2</sub>, R2=C<sub>11</sub>N<sub>2</sub>O<sub>4</sub>H<sub>13</sub>



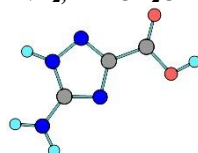
L



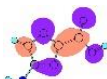
H



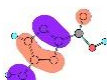
T2: R1=NH<sub>2</sub>, R2=CH<sub>2</sub>O



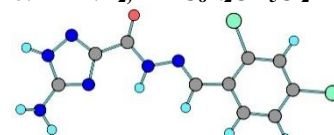
L



H



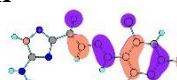
T10: R1=NH<sub>2</sub>, R2=C<sub>8</sub>N<sub>2</sub>O<sub>5</sub>Cl<sub>2</sub>



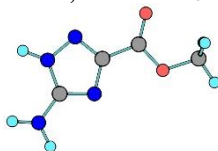
L



H



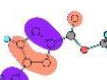
T3: R1=NH<sub>2</sub>, R2=C<sub>2</sub>O<sub>2</sub>H<sub>3</sub>



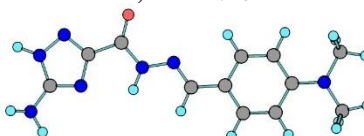
L



H



T11: R1=NH<sub>2</sub>, R2=C<sub>10</sub>N<sub>3</sub>O<sub>3</sub>H<sub>12</sub>



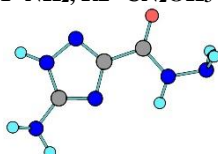
L



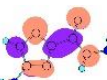
H



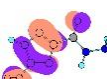
T4: R1=NH<sub>2</sub>, R2=CN<sub>2</sub>OH<sub>3</sub>



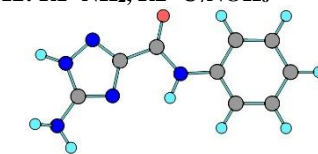
L



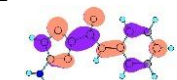
H



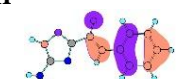
T12: R1=NH<sub>2</sub>, R2=C<sub>7</sub>NO<sub>6</sub>H<sub>6</sub>



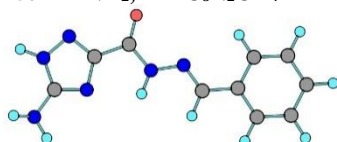
L



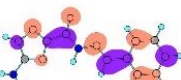
H



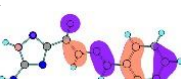
T5: R1=NH<sub>2</sub>, R2=C<sub>8</sub>N<sub>2</sub>O<sub>7</sub>H<sub>7</sub>



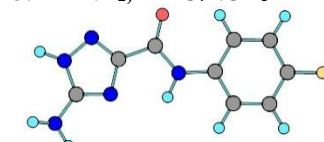
L



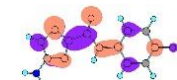
H



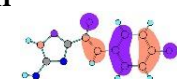
T13: R1=NH<sub>2</sub>, R2=C<sub>7</sub>NO<sub>5</sub>H<sub>5</sub>F



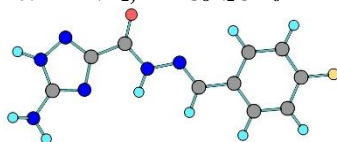
L



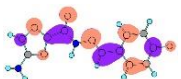
H



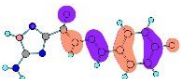
T6: R1=NH<sub>2</sub>, R2=C<sub>8</sub>N<sub>2</sub>O<sub>6</sub>H<sub>6</sub>F



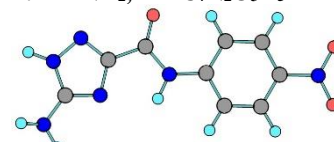
L



H



T14: R1=NH<sub>2</sub>, R2=C<sub>7</sub>N<sub>2</sub>O<sub>3</sub>H<sub>5</sub>



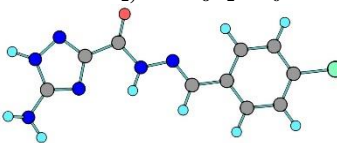
L



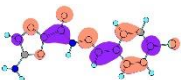
H



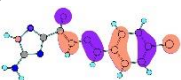
T7: R1=NH<sub>2</sub>, R2=C<sub>8</sub>N<sub>2</sub>O<sub>6</sub>H<sub>6</sub>Cl



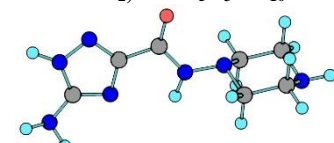
L



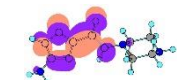
H



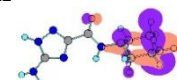
T15: R1=NH<sub>2</sub>, R2=C<sub>5</sub>N<sub>3</sub>O<sub>3</sub>H<sub>10</sub>



L



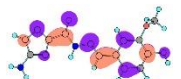
H



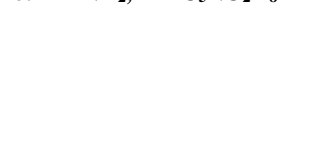
T8: R1=NH<sub>2</sub>, R2=C<sub>9</sub>N<sub>2</sub>O<sub>3</sub>H<sub>9</sub>



L



T16: R1=NH<sub>2</sub>, R2=C<sub>5</sub>NO<sub>2</sub>H<sub>8</sub>



L



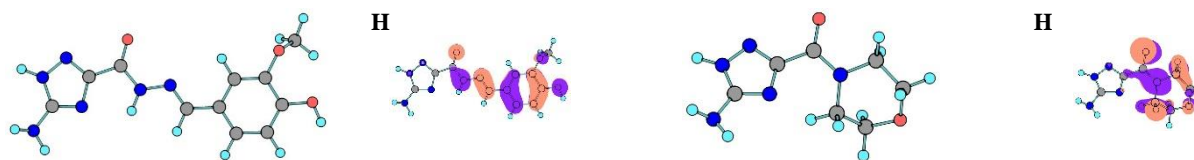


**Figure 2.** Representations of the optimized ligand models and HOMO/LUMO patterns (H/L).

**Table 1.** The evaluated energetic features of the models.<sup>1</sup>

Ligand	HOMO eV	LUMO eV	E <sub>Gap</sub> eV	CH eV	CS eV <sup>-1</sup>	Score kcal/mol	Rank
T1	-7.38	0.13	7.52	3.76	0.27	-61.1	16
T2	-6.26	-0.75	5.51	2.75	0.36	-95.88	14
T3	-6.17	-0.62	5.56	2.78	0.36	-95.83	15
T4	-6.56	-0.52	6.04	3.02	0.33	-100.35	13
T5	-5.77	-1.34	4.42	2.21	0.45	-124.95	8
T6	-5.78	-1.39	4.39	2.20	0.46	-133.67	4
T7	-5.89	-1.55	4.33	2.17	0.46	-132.05	6
T8	-5.42	-1.19	4.23	2.12	0.47	-153.27	1
T9	-5.47	-1.29	4.18	2.09	0.48	-137.48	2
T10	-6.02	-1.69	4.33	2.16	0.46	-125.99	7
T11	-4.84	-0.96	3.88	1.94	0.52	-133.06	5
T12	-5.71	-0.85	4.86	2.43	0.41	-110.45	12
T13	-5.71	-0.91	4.79	2.40	0.42	-115.44	10
T14	-6.48	-2.18	4.31	2.15	0.46	-133.82	3
T15	-6.02	-0.33	5.69	2.85	0.35	-113.95	11
T16	-6.25	-0.38	5.87	2.93	0.34	-120.72	9

<sup>1</sup>The models were shown in Figures 2 and 3. HOMO: the highest occupied molecular orbital, LUMO: the lowest unoccupied molecular orbital, E<sub>Gap</sub>: energy gap between HOMO and LUMO, CH: chemical hardness, CS: chemical softness, Score: molecular docking score, Rank: priority of ligands for interactions with the target based on the obtained scores.

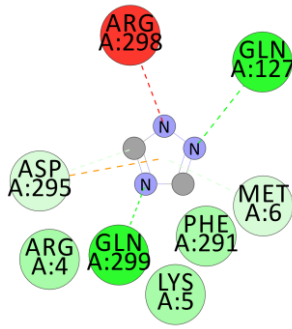
### 3. Results and Discussion

This work investigated fifteen models of derivatives of 1,2,4-triazole for involvement in interactions with the MPro of coronavirus through the *in silico* media. The models' derivatives were listed as T2-T16 based on the types of substituted molecular groups to each of R1 and R2 shown 1,2,4-triazole of Figure 1. In the original T1 model, both R1 and R2 were substituted by the hydrogen atoms, whereas they were substituted with other molecular groups in the rest of the T2-T16 models, as shown in Figure 2. The ligand models were optimized to yield the stabilized forms of T1-T16 as the investigating ligands for involvement in the interactions with the MPro target of coronavirus. As shown in Figure 2, R1 was fixed in whole T2-T16 models with a substituted -NH<sub>2</sub> group, whereas different substituted R2 groups varied the models. It should be mentioned that the current ligand models were synthesized before and were proposed for working in biological systems [32]. Therefore, they were investigated in this work to assess their potential for interacting with the MPro of coronavirus for approaching the inhibition of enzymatic activity. The stabilized models of T1-T16 showed structural variations of R1 and R2 substitutions. Their obtained configurations provided possibilities for examinations of different structural geometries for involvement in the interactions with a macromolecular target. To this point, the models were provided regarding the stabilized features. Next, the graphical distribution patterns of HOMO and LUMO indicated variations of electronic molecular orbitals features among the ligand models, in which the localization of patterns was different in the stabilized models. Although the core structure of all models was the same, substituting the additional molecular groups yielded different features for the products. In this regard, the observed HOMO and LUMO distributions showed the benefits of employing such molecular modifications to obtain the models' specific electronic features for further use. The results of Table 1 also indicated such variations in the quantitative scale, in which the levels of HOMO and LUMO were changed in T1-T16 model systems. As

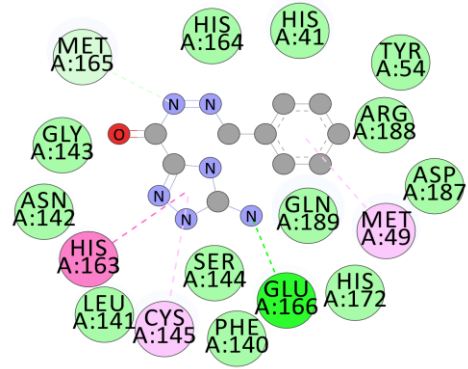
known for the electron-occupied level of HOMO and electron-unoccupied level of LUMO, HOMO could stand for a level of electron donor, and LUMO could stand for a level of electron acceptor. Accordingly, their participation in future interactions with other substances will be changed due to the existence of different HOMO and LUMO levels. A general achievement on the obtained values of HOMO and LUMO of T1-T16 could reveal that the levels of HOMO and LUMO were closer to each other in T2-T16 derivatives in comparison with the original T1 model. This trend could be emphasized by obtaining a higher activity for the derivatives for involving in interactions with other substances. The values of E<sub>Gap</sub>, standing for the energy gap between HOMO and LUMO, indicated smaller values for the derivatives in comparison with T1. As a consequence, the values of CH, chemical hardness, were decreased for the models, and the values of CS, chemical softness, were increased. In this regard, the employed modification of models was assumed to be more interactive with other substances based on their characteristic electronic features. To assess such achievement, molecular docking simulations were performed to recognize the tendency of ligand models to interact with the MPro target to create the ligand-target complexes, as shown in Figure 3.

A molecular docking simulation is a tool of *in silico* media for investigating details of interactions of ligand-target complexes. Accordingly, this tool was employed in this work to recognize interactions between each of the T1-T16 ligand models and the MPro target of coronavirus. As mentioned earlier, the ligand models showed characteristic structural and electronic features regarding the modification of R1 and R2 groups of 1,2,4-triazole. Hence, their interaction features were also investigated in this part of the current research work to learn about their potential for inhibition of the activity of the MPro target. As shown in Figure 3, each ligand interacted with a collection of amino acids of MPro, as indicated by the disk shapes around the central ligand structure. Such interactions occurred by a mixture of physical types of interactions, including hydrogen bond and non-hydrogen bond interactions. The green color dash lines showed the hydrogen bond interactions, the cyan color showed van der Waals interactions, pi-types of interactions were shown in the violet color, and an unsuitable interaction was shown by the red color. Consequently, the models of bimolecular T...Mpro complexes were stabilized by performing molecular docking simulations to show the numbers and types of interactions involving each T ligand and the MPro target. Returning to the results of ligand models, observation of different interaction features was expected for each ligand versus the MPro target. Accordingly, different interaction environments were observed for the complexes of each ligand and the target. The evaluated molecular docking scores were summarized in Table 1 to show the strength of such interacting complex formation and to compare the potential of each ligand for participating in a more efficient interaction with the target. Additionally, comparing the current results with those of other works [13-18] indicated reasonable potentials of all T1-T16 ligand models for interacting with the MPro target of coronavirus for approaching a possible inhibition of enzymatic activity. In this regard, the models were ranked for showing the ligands with their potency of involvement in interactions. T8 was the ligand with the highest potency of interactions, and T1 was the ligand with the lowest potency of interactions with the MPro target. Here with this observation, the idea of structural modification of 1,2,4-triazole for achieving better-interacting ligands was affirmed based on the higher scores of all T2-T16 ligands compared to the T1 ligand. Accordingly, the rest of the ligand models were recognized by their scores in this way: T8 > T9 > T14 > T6 > T11 > T7 > T10 > T5 > T16 > T13 > T15 > T12 > T4 > T2 > T3 > T1.

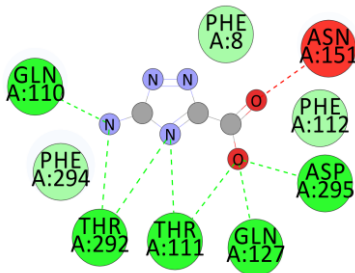
T1...MPro



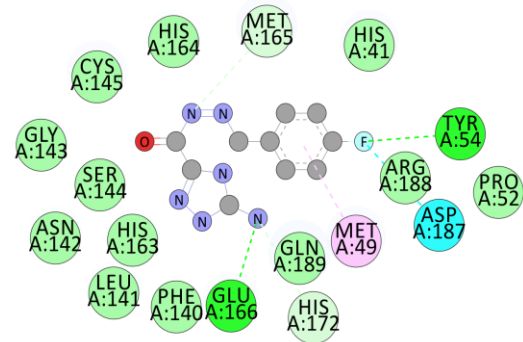
T5...MPro



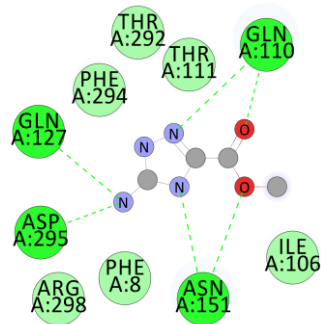
T2...MPro



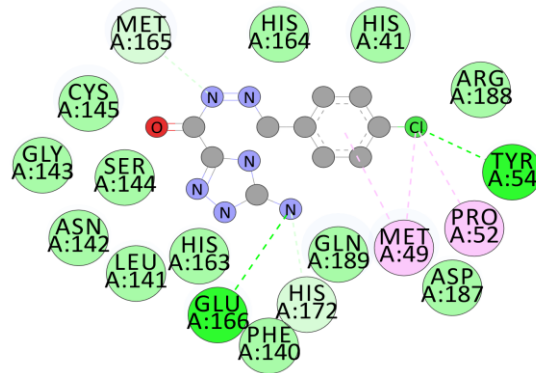
T6...MPro



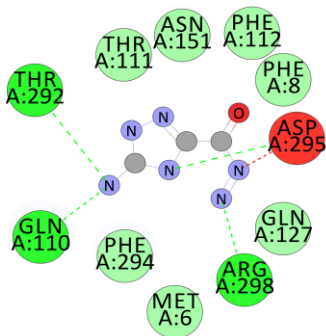
T3...MPro



T7...MPro



T4...MPro



T8...MPro

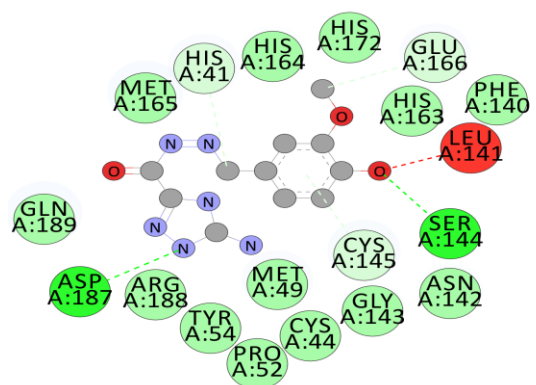
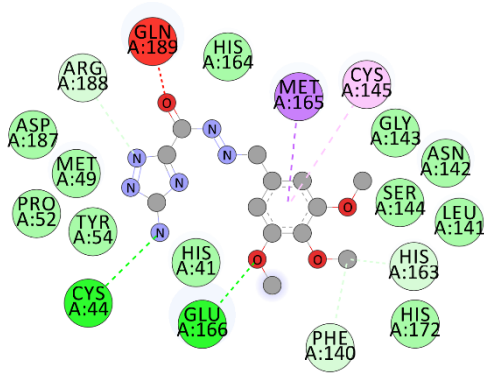
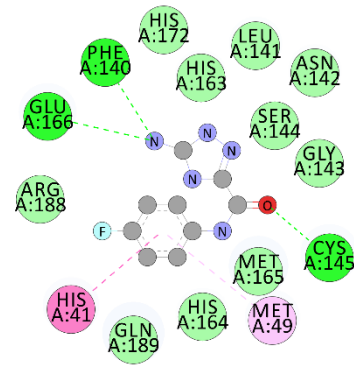


**Figure 3.** Representations of the ligand...target interactions; Part 1: T1-T8.

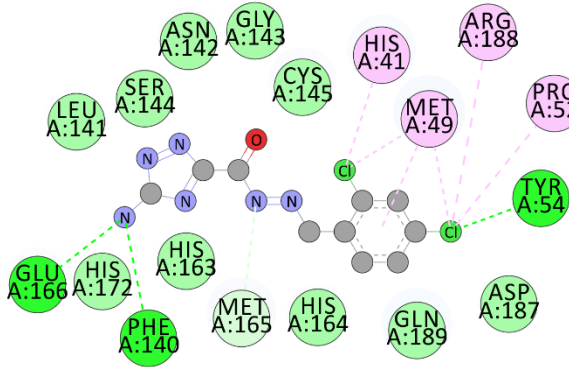
T9...MPro



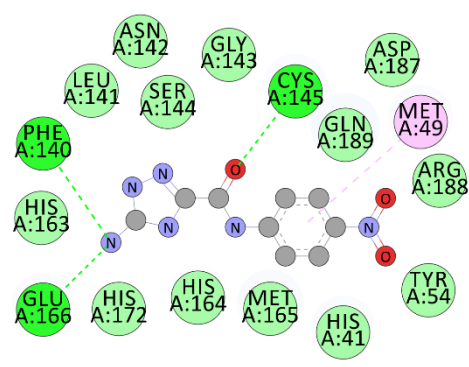
T13...MPro



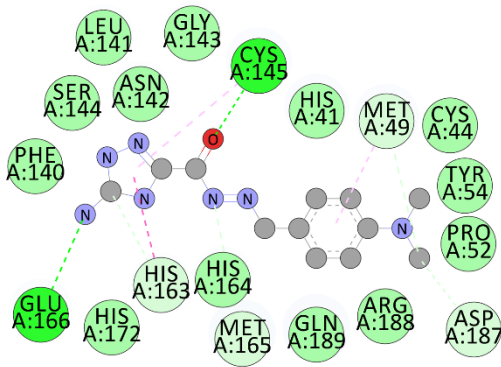
T10...MPro



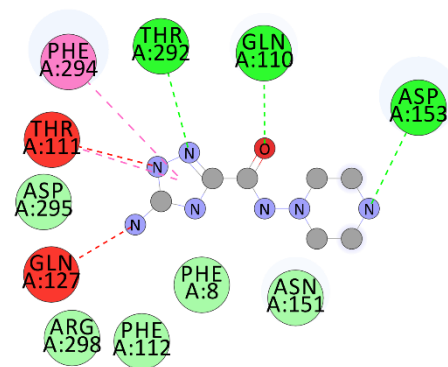
T14...MPro



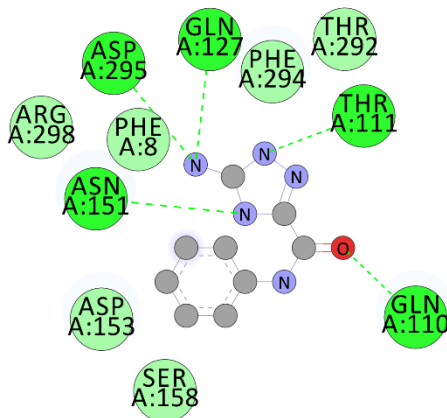
T11...MPro



T15...MPro



T12...MPro



T16...MPro

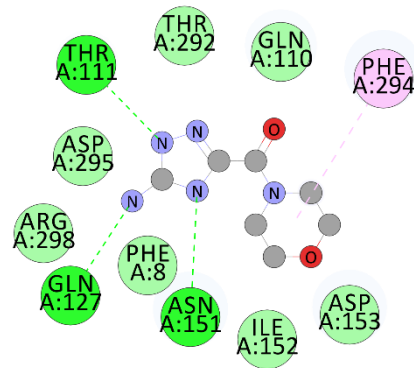


**Figure 3 (Continued).** Representations of the ligand...target interactions; Part 2: T9-T16.

To interpret such observation, it could be mentioned that the ligand models were involved in interactions based on their suitable interacting molecular and atomic sites and were more or less in comparison with each other. By examining the attached molecular groups, the

results showed the potency of T8 for involvement in more efficient interaction with the MPro target. In Figure 2 and Figure 3, the graphical features of T8 were exhibited to learn this model's structural and electronic advantages compared with other models. For drug design issues, the structure-activity relationship (SAR) emphasizes the impacts of structural features on the corresponding activity of a ligand. Hence, learning the characteristic features of ligands could help to make them appropriate for specific activity applications, in which such SAR issues could also examine further modifications of the models. Accordingly, new molecular molecules could be recognized for showing specific applications [37-40].

Comparing the interacting representations of T...Mpro complexes (Figure 3) could show the specification of each ligand for involvement in interactions with the corresponding amino acids. Although some amino acids are observed for almost all of the interacting models, the types of interactions and the involving site of ligands for participating in interactions are both different. In this regard, the ligand models could be specified regarding the desired mode of interaction with the target to show the drug design, discovery, and development routes.

#### 4. Conclusions

Within this work, *in silico* interactions of some of the 1,2,4-triazole derivatives with the MPro of coronavirus were investigated to approach insights into the inhibition of the enzymatic activity. The results indicated that all the investigated T2-T16 derivatives were working better than the original T1 ligand structure in interaction with the MPro target. By performing DFT calculations, the stabilized ligand models indicated different structural and electronic features showing the impacts of modifications of the original ligand to achieve specified results. Moreover, the ligand interacted with the MPro target in different potency levels, in which the bimolecular T...MPro complex models were obtained by performing molecular docking simulations. Consequently, the obtained different features of ligands yielded different modes of interactions between the ligands and the target, in which the achievement could emphasize the benefits of modifying the structures to approach more efficient results. To summarize this work regarding its major problem, it could be mentioned that the investigated 1,2,4-triazole derivatives could be expected to work as potent inhibitors of MPro of coronavirus.

#### Funding

This research received a funding grant (no. 199551) from the Student Research Committee of the Research Council of Isfahan University of Medical Sciences.

#### Acknowledgments

E.S. acknowledges the support of the Student Research Committee of the Research Council of Isfahan University of Medical Sciences.

#### Conflicts of Interest

The authors declare no conflict of interest.

#### References

1. Selmi, A.; Zarei, A.; Tachoua, W.; Puschmann, H.; Teymourinia, H.; Ramazani, A. Synthesis and structural analysis of a novel stable quinoline dicarbamic acid: x-ray single crystal structure of (2-((4-((2-(carboxy(methyl)amino)ethoxy)carbonyl) quinoline-2-yl)oxy) ethyl) (methyl)-carbamic acid and molecular <https://biointerfaceresearch.com/>

- docking assessments to test its inhibitory potential against SARS-CoV-2 main protease. *Chemical Methodologies* **2022**, *6*, 463–474, <https://doi.org/10.22034/chemm.2022.335353.1462>.
2. Hussain, S.; Alsinai, A.; Afzal, D.; Maqbool, A.; Afzal, F.; Cancan, M. Investigation of closed formula and topological properties of remdesivir (C27H35N6O8P). *Chemical Methodologies* **2021**, *5*, 485–497, <https://doi.org/10.22034/chemm.2021.138611>.
  3. Darvishzadeh, A.; Hasani, H.; Behrouzinezhad, R.; Bahmani, A.; Delavar, M. Evaluation of predictors of mortality in patients with COVID-19: a systematic review and meta-analysis. *Eurasian Chemical Communications* **2022**, *4*, 392–401, <https://doi.org/10.22034/ecc.2022.323511.1292>.
  4. Shyam, T.; Das, S. Impact of Covid-19 on education scenario and digital divide in India. *Eurasian Chemical Communications* **2021**, *3*, 700–705, <https://doi.org/10.22034/ecc.2021.294584.1201>.
  5. Nourmohammadi, J.; Jafari, M.; Abbaszadeh, R.; Rahimi Ghasabeh, S.; Amani, H.; Kalali Sani, S. Chest CT findings in patients with COVID-19 infection: a systematic review and meta-analysis. *Eurasian Chemical Communications* **2022**, *4*, 425–431, <https://doi.org/10.22034/ecc.2022.329086.1323>.
  6. Casaroto, A.R.; Jamali, J.; Amini, F.; Talebzade Toranji, M.; Kayasöken, G. Evaluating epidemiology, symptoms, and routes of COVID-19 for dental care: a literature review. *International Journal of Scientific Research in Dental and Medical Sciences* **2020**, *2*, 37–41, <https://doi.org/10.30485/ijrdms.2020.231680.1056>.
  7. Jamali, S.; Marcella, C.; Prakash, P.; Moradkhani, A.; Kasraei, E. Prevalence of malignancy and chronic obstructive pulmonary disease among patients with COVID-19: a systematic review and meta-analysis. *International Journal of Scientific Research in Dental and Medical Sciences* **2020**, *2*, 52–58, <https://doi.org/10.30485/ijrdms.2020.233746.1062>.
  8. Munipati, S.; Rachamadugu, H.; Avileli, S.; Avula, R.; Beladona, N.J.; Boyapally, S.R. Microbiological profile of post-COVID-19 mucormycosis in various samples. *International Journal of Scientific Research in Dental and Medical Sciences* **2022**, *4*, 87–91, <https://doi.org/10.30485/ijrdms.2022.338567.1285>.
  9. Asefy, Z.; Mammadova, S.; Nasibova, A.; Khalilov, R.; Aliyev, E.; Zhdanov, R.; Eftekhari, A. Post corona: chemicals, environmental factors, and public health. *Eurasian Chemical Communications* **2021**, *3*, 526–532, <https://doi.org/10.22034/ecc.2021.293309.1195>.
  10. Nguyen, T.T.; Jung, J.H.; Kim, M.K.; Lim, S.; Choi, J.M.; Chung, B.; Kim, D.W.; Kim, D. The inhibitory effects of plant derivate polyphenols on the main protease of SARS coronavirus 2 and their structure–activity relationship. *Molecules* **2021**, *26*, 1924, <https://doi.org/10.3390/molecules26071924>.
  11. Aponte Mendez, M.; Rivera Marval, E.K.; Talebzade Toranji, M.; Amini, F.; Casaroto, A.R. Dental care for patients during the Covid-19 outbreak: a literature review. *International Journal of Scientific Research in Dental and Medical Sciences* **2020**, *2*, 42–45, <https://doi.org/10.30485/ijrdms.2020.232096.1058>.
  12. Hundekari, J.; Mittal, R.; Wasnik, S.; Kot, L. Perception of equivalence between online and face-to-face academic activities by undergraduate medical students during COVID-19 Pandemic. *International Journal of Scientific Research in Dental and Medical Sciences* **2020**, *2*, 115–120, <https://doi.org/10.30485/ijrdms.2020.253310.1091>.
  13. Harismah, K.; Hajali, N.; Mirzaei, M.; Salarzaei, E. Quantum processing of cytidine derivatives and evaluating their in silico interactions with the COVID-19 main protease. *Main Group Chemistry* **2022**, *21*, 263–270, <https://doi.org/10.3233/mgc-210134>.
  14. Pandey, A.K.; Singh, V.; Dwivedi, A. Comparative study of molecular docking, structural, electronic, vibrational and hydrogen bonding interactions on 4-hydroxy benzo hydrazide (4HBH) and its newly designed derivative [(E)-N'-((1H-Pyrrol-2-YL)methylene)-4-hydroxy benzo hydrazide and its isomers (I, II and III)](potential inhibitors) for COVID-19 protease. *Main Group Chemistry* **2021**, *20*, 295–315, <https://doi.org/10.3233/mgc-210039>.
  15. Chia, C.B.; Xu, W.; Shuyi Ng, P. A patent review on SARS coronavirus main protease (3CLpro) inhibitors. *ChemMedChem* **2022**, *17*, e202100576, <https://doi.org/10.1002/cmdc.202100576>.
  16. Zhang, Y.; Gao, H.; Hu, X.; Wang, Q.; Zhong, F.; Zhou, X.; Lin, C.; Yang, Y.; Wei, J.; Du, W.; Huang, H. Structure-based discovery and structural basis of a novel broad-spectrum natural product against the main protease of coronavirus. *Journal of Virology* **2022**, *96*, e01253–21, <https://doi.org/10.1128/JVI.01253-21>.
  17. Elekofehinti, O.O.; Iwaloye, O.; Famusiwa, C.D.; Akinseye, O.; Rocha, J.B. Identification of main protease of coronavirus SARS-CoV-2 (Mpro) inhibitors from *Melissa officinalis*. *Current Drug Discovery Technologies* **2021**, *18*, 38–52, <https://doi.org/10.2174/1570163817999200918103705>.

18. Sargolzaei, M. Effect of nelfinavir stereoisomers on coronavirus main protease: molecular docking, molecular dynamics simulation and MM/GBSA study. *Journal of Molecular Graphics and Modelling* **2021**, *103*, 107803, <https://doi.org/10.1016/j.jmgm.2020.107803>.
19. Ahmed, S.; Salau, S.; Khan, A.; Saeed, M.; Ul-Haq, Z. Inhibitive property of catechin and chlorogenic acid against human pancreatic lipase: mMolecular docking and molecular dynamics simulation investigations. *Advanced Journal of Chemistry-Section A* **2022**, *5*, 226–240, <https://doi.org/10.22034/ajca.2022.338380.1311>.
20. Olaleye, O.; Oladipupo, A.; Oyawaluja, B.; Coker, H. Chemical composition, antioxidative and antimicrobial activities of different extracts of the leaves of *Parquetina nigrescens* (Asclepiadaceae). *Progress in Chemical and Biochemical Research* **2021**, *4*, 359–371, <https://doi.org/10.22034/pcbr.2021.287025.1188>.
21. Alizadeh, S.; Nazari, Z. Amphetamine, methamphetamine, morphine @ AuNPs kit based on PARAFAC. *Advanced Journal of Chemistry-Section A* **2022**, *5*, 253–262, <https://doi.org/10.22034/ajca.2022.345350.1318>.
22. Ejeh, S.; Uzairu, A.; Shallangwa, G.; Abechi, S.; Ibrahim, M. In silico identification of some novel ketoamides as potential pan-genotypic HCV NS3/4A protease inhibitors with drug-likeness, pharmacokinetic ADME profiles and synthetic accessibility predictions. *Advanced Journal of Chemistry-Section A* **2022**, *5*, 197–207, <https://doi.org/10.22034/ajca.2022.329332.1302>.
23. Wikantyasning, E.R.; Kalsum, U.; Nurfiani, S.; Da'I, M.; Cholisoh, Z. Allylamine-conjugated polyacrylic acid and gold nanoparticles for colorimetric detection of bacteria. *Materials Science Forum* **2021**, *1029*, 137–144, <https://doi.org/10.4028/www.scientific.net/msf.1029.137>.
24. Wikantyasning, E.R.; Mutmainnah, M.; Cholisoh, Z.; Hairunisa, I.; Bakar, M.F.A.; Da'i, M. Preparation of hydrogel nanocomposite containing gold nanoparticles with unique swelling/deswelling properties. *Rasayan Journal of Chemistry* **2019**, *12*, 1857–1863, <https://doi.org/10.31788/rjc.2019.1245209>.
25. Kausikan, S.P.; Anu, S.; Saravanan, M.; Devisri, T.; Rekha, K.; John, R. The impact of COVID-19 on auditory and visual choice reaction time of non-hospitalized patients: an observational study. *International Journal of Scientific Research in Dental and Medical Sciences* **2022**, *4*, 21–25, <http://doi.org/10.30485/ijrdms.2022.327884.1250>.
26. Baghizadeh Fini, M. Transmission routes of SARS-CoV-2 in dentistry: a literature review. *International Journal of Scientific Research in Dental and Medical Sciences* **2020**, *2*, 135–137, <https://doi.org/10.30485/ijrdms.2020.252402.1088>.
27. Verma, I.; Kumar, A.; Antony, J.; Ansari, S.A.; Kaushal, R.; Rajput, D.P. Study of clinical profile of COVID-19 patients with respect to COVID-19 vaccination status: an analytical study from a tertiary care center in India. *International Journal of Scientific Research in Dental and Medical Sciences* **2022**, *4*, 57–66, <https://doi.org/10.30485/ijrdms.2022.339254.1289>.
28. Chu, X.M.; Wang, C.; Wang, W.L.; Liang, L.L.; Liu, W.; Gong, K.K.; Sun, K.L. Triazole derivatives and their antiplasmodial and antimalarial activities. *European Journal of Medicinal Chemistry* **2019**, *166*, 206–223, <https://doi.org/10.1016/j.ejmech.2019.01.047>.
29. Staśkiewicz, A.; Ledwoń, P.; Rovero, P.; Papini, A.M.; Latajka, R. Triazole-modified peptidomimetics: an opportunity for drug discovery and development. *Frontiers in Chemistry* **2021**, *9*, 674705, <https://doi.org/10.3389/fchem.2021.674705>.
30. Song, M.X.; Deng, X.Q. Recent developments on triazole nucleus in anticonvulsant compounds: a review. *Journal of Enzyme Inhibition and Medicinal Chemistry* **2018**, *33*, 453–478, <https://doi.org/10.1080/14756366.2017.1423068>.
31. Baharloui, M.; Mirshokraee, S.A.; Monfared, A.; Tehrani, M.H. Design and synthesis of novel triazole-based peptide analogues as anticancer agents. *Iranian Journal of Pharmaceutical Research* **2019**, *18*, 1299–1308, <https://doi.org/10.22037/ijpr.2019.111722.13320>.
32. Amin, N.H.; El-Saadi, M.T.; Ibrahim, A.A.; Abdel-Rahman, H.M. Design, synthesis and mechanistic study of new 1, 2, 4-triazole derivatives as antimicrobial agents. *Bioorganic Chemistry* **2021**, *111*, 104841, <https://doi.org/10.1016/j.bioorg.2021.104841>.
33. Lin, X.; Li, X.; Lin, X. A review on applications of computational methods in drug screening and design. *Molecules* **2020**, *25*, 1375, <https://doi.org/10.3390/molecules25061375>.
34. Frisch, M.J.; Trucks, G.W.; Schlegel, H.B. et al. Gaussian 09 program. *Gaussian Inc.* **2009**, Wallingford, CT.
35. Jin, Z.; Du, X.; Xu, Y. et al. Structure of Mpro from SARS-CoV-2 and discovery of its inhibitors. *Nature* **2020**, *582*, 289–293, <http://doi.org/10.1038/s41586-020-2223-y>.

36. Yan, Y.; Tao, H.; He, J.; Huang, S.Y. The HDock server for integrated protein–protein docking. *Nature Protocols* **2020**, *15*, 1829–1852, <https://doi.org/10.1038/s41596-020-0312-x>.
37. Hote, B.; Muley, D.B.; Mandawad, G.G. Simple and efficient synthesis of 2-styryl-4H-chromone-4-one derivatives by modification of the Baker-Venkataraman method. *Journal of Applied Organometallic Chemistry* **2021**, *1*, 9–16, <https://doi.org/10.22034/jaoc.2021.275519.1001>.
38. Sharma, G.; Sharma, S.B. Synthetic impatiol analogues as potential cyclooxygenase-2 inhibitors: a preliminary study. *Journal of Applied Organometallic Chemistry* **2021**, *1*, 66–75, <https://doi.org/10.22034/jaoc.2021.276815.1006>.
39. Mezoughi, A.; Mohammed, W.; Ettarhouni, Z.O. Recent biological applications and chemical synthesis of thiohydantoin. *Journal of Chemical Reviews* **2021**, *3*, 196–218, <https://doi.org/10.22034/jcr.2021.285244.1111>.
40. Peddagundam, B.; Abdul Ahad, H.; Chinthaginjala, H.; Ksheerasagare, T.; Ganthala, A.K.; Gummadisani, G.R. The design of soft drugs: basic principles, energetic metabolite methods, approved compounds, and pharmaceutical applications. *Journal of Chemical Reviews* **2022**, *4*, 241–254, <https://doi.org/10.22034/jcr.2022.336306.1164>.